High-temperature expansion of the magnetic susceptibility and higher moments of the correlation function for the two-dimensional *XY* model

H. Arisue*

Osaka Prefectural College of Technology, 26-12 Saiwai-cho, Neyagawa, Osaka 572, Japan

(Received 29 July 2008; published 8 January 2009)

We calculate the high-temperature series of the magnetic susceptibility and the second and fourth moments of the correlation function for the *XY* model on the square lattice to order β^{33} by applying the improved algorithm of the finite lattice method. The long series allow us to estimate the inverse critical temperature as $\beta_c=1.1200(1)$, which is consistent with the most precise value given previously by the Monte Carlo simulation. The critical exponent for the multiplicative logarithmic correction is evaluated to be $\theta=0.054(10)$, which is consistent with the renormalization group prediction of $\theta=\frac{1}{16}$.

DOI: 10.1103/PhysRevE.79.011107 PACS number(s): 05.50.+q, 64.60.Cn, 75.10.Hk, 75.40.Cx

I. INTRODUCTION

It is believed that the *XY* model in two dimensions exhibits a phase transition of the Kosterlitz-Thouless (KT) type [1], which is driven by the condensation of vortices. From the renormalization group arguments, it was predicted that the correlation length has an essential singularity at the transition temperature T_c as

$$\xi \sim \exp\left(\frac{b}{t^{\sigma}}\right), \tag{1}$$

with $\sigma=\frac{1}{2}$ where $t=T/T_c-1$ is the reduced temperature and b is a nonuniversal constant. At the critical temperature the correlation function for the two spins with the distance r behaves as

$$G(r) \sim \frac{(\ln r)^{2\theta}}{r^{\eta}}\left[1+O\left(\frac{\ln\ln r}{\ln r}\right)\right], \tag{2}$$

with $\eta=\frac{1}{4}$ and $\theta=\frac{1}{16}$ when $r\to\infty$, and the behavior of the jth moment m_j of the correlation function near the critical temperature is

$$m_j \sim \xi^{2+j-\eta}(\ln \xi)^{2\theta}\left[1+O\left(\frac{\ln\ln \xi}{\ln \xi}\right)\right]. \tag{3}$$

The free energy and its temperature derivatives (i.e., the internal energy and the specific heat) were also predicted to behave as

$$f \sim \xi^{-2} + \text{nonsingular term}. \tag{4}$$

At the critical temperature, the first term on the right-hand side of Eq. (4) has an essential singularity with itself and its derivatives going to zero, while the second term stays nonzero.

The behavior in Eq. (1) for the correlation length has been well established both by numerical simulations and the high-temperature expansion. The standard Monte Carlo simulation [2,3] gave $\beta_c=1.130(15)$ with $b=2.15(10)$ and $\beta_c=1.118(5)$ with $b=1.70(20)$ for the square lattice. (Here β_c is the critical inverse temperature, which will be defined below.) More precise values $\beta_c=1.1208(2)$ with $b=1.800(2)$ [4] and $\beta_c=1.1199(1)$ with $b=1.776(4)$ [5] were obtained using the finite-size scaling technique and the renormalization group finite-size scaling method, respectively. In the latter approach, the renormalization group flow of the observable was matched with that of the exactly solvable BCSOS model. The latter value of β_c was recently confirmed by a large scale Monte Carlo simulation on a 2048×2048 lattice using the finite-size scaling method [6]. On the other hand, the high-temperature expansion for the magnetic susceptibility and higher moments of the correlation function to order β^{21} [7] and β^{26} [8] gave less precise value $\beta_c=1.118(3)$ with $b=1.67(4)$ and $\beta_c=1.1198(14)$ with $b=1.77(1)$, respectively. It seems that the available high-temperature series is not long enough to give the estimation of the values for the critical temperature and other critical parameters to the same precision as the Monte Carlo simulation. So it is desirable to extend the high-temperature series to much higher order.

As for the critical exponent θ for the multiplicative logarithmic correction in the moments of the correlation function, there has been controversial arguments. Negative values ranging from $\theta=-0.077$ to $\theta=-0.056$ [9–11] were given by the analysis of the numerical simulation based on the thermal scaling formula (3), while the finite size scaling analysis gave positive values in the range of $\theta=0.02-0.035$ [10–13]. The large scale Monte Carlo simulation by Hasenbusch [6] gave a value $\theta=0.056(7)$, which is consistent with the renormalization group prediction, assuming a modified finite-size-scaling behavior

$$m_0 \sim L^{2-\eta}(C+\ln L)^{2\theta}, \tag{5}$$

where L is the size of the lattice used in the simulation and C is a constant. On the other hand, the high-temperature expansion series to order β^{21} [7] gave negative values of $\theta=-0.042(5)$ from the combination of the susceptibility and the second moment correlation length and $\theta=-0.05(2)$ from the combination of the fourth moment of the correlation function and the second moment correlation length, assuming the thermal scaling (3). We should note that these values from the high-temperature series are obtained only for the Dlog-Padé approximants and the general inhomogeneous differential approximants do not give convergent result to

*arisue@ipc.osaka-pct.ac.jp

this order. Higher order series would be needed again to resolve the discrepancy between the result of the high-temperature series analysis and the renormalization group prediction.

A commonly known method for series expansions is the graphical method [14]. However, in this method, one must list all the graphs that contribute to the desired order of the series. An alternative and powerful method to generate the expansion series is the finite lattice method [15–17]. It avoids listing all the graphs and it reduces the problem to the calculation of the partition functions for the relevant finite-size lattices, which is a rather straightforward procedure if we use the transfer matrix formulation. In many cases, the finite lattice method generates longer series than the graphical method [18–25]. Unfortunately, in the case of the *XY* model in two dimensions, the original finite lattice method can generate a high-temperature series that is at most as long as the series that can be obtained by the graphical method.

In order to generate long series for the the *XY* model in two dimensions, we here apply an improved algorithm of the finite lattice method developed by the author and Tabata [26,27]. This improved algorithm is powerful in the case of models in which the spin variable at each site takes more than two values, including an infinite number of values. This algorithm was applied to generate a low-temperature series for the solid-on-solid model [26] and high- and low-temperature series for the q-state Potts model in two dimensions [27]. In both cases, it generates much longer series than the original finite lattice method. The *XY* model in two dimensions can be mapped to a kind of solid-on-solid model, and the improved algorithm of the finite lattice method in fact enabled us to obtain the high-temperature series for the free energy of this model on the square lattice to order β^{48} [28], which is two times longer than the series previously derived. From the analysis of the long series we confirmed that the free energy of the two-dimensional *XY* model behaves similar to Eq. (4), with values of the critical temperature and the nonuniversal constant b that are close to the values obtained in the study of the correlation length. We apply this improved algorithm of the finite lattice method to generate the high-temperature series to order β^{33} for the magnetic susceptibility and the second and fourth moments of the correlation function. The long series will provide the value of the critical temperature to the same precision as the latest large scale Monte Carlo simulations and the value of the critical exponent θ which is consistent with the renormalization group prediction.

In Sec. II, we describe how to apply the improved algorithm of the finite lattice method to generate the high-temperature series for the moments of the correlation function. In Sec. III, the high-temperature series to order β^{33} are given. Sec. IV is devoted to the analysis of the obtained series to evaluate the critical parameters.

II. ALGORITHM

We consider the *XY* model defined on the square lattice. The Hamiltonian of this system is

$$H = -\sum_{\langle i,j\rangle} J\vec{s}_i \cdot \vec{s}_j, \tag{6}$$

where $\vec{s}_i$ is a two-dimensional unit vector located at the lattice site i, and the summation is taken over all pairs $\langle i,j\rangle$ of nearest neighbor sites. The correlation function is given by

$$\langle \vec{s}_x \cdot \vec{s}_0 \rangle = \frac{\Gamma_{x,0}}{Z}, \tag{7}$$

where Z is the partition function

$$Z = \int \prod_i d\theta_i \exp\left(-\frac{H}{kT}\right), \tag{8}$$

and

$$\Gamma_{x,0} = \int \prod_i d\theta_i \vec{s}_x \cdot \vec{s}_0 \exp\left(-\frac{H}{kT}\right). \tag{9}$$

Here T is the temperature and θ_i is the angle variable of the spin $\vec{s}_i = (\cos\theta_i, \sin\theta_i)$.

This model can be mapped exactly to a solid-on-solid model and the numerator and denominator of Eq. (9) can be rewritten as

$$Z = \sum_{\{h|-\infty \le h_i \le +\infty\}} \prod_{\langle i,j\rangle} I_{|h_i - h_j|}(\beta) \tag{10}$$

and

$$\Gamma_{x,0} = \sum_{\{h|-\infty \le h_i \le +\infty\}} \prod_{\langle i,j\rangle} I_{|h_i - h_j + \Delta_{i,j;x,0}|}(\beta), \tag{11}$$

where $\beta = J/kT$, I_n is the modified Bessel function, the product is taken with respect to all the pairs of neighboring plaquettes, and the variable h_i at each plaquette i takes integer values ranging from $-\infty$ to $+\infty$. In Eq. (11) the $\Delta_{i,j;x,0}$ is defined as

$$\Delta_{i,j;x,0} = \begin{cases} 1 & \text{for } b_{i,j} \in L_{x,0}, \\ 0 & \text{otherwise}, \end{cases} \tag{12}$$

where $b_{i,j}$ is the bond sandwiched by the neighboring plaquettes i and j, and $L_{x,0}$ is the set of bonds on an arbitrary shortest path connecting the sites $0=(0,0)$ and $x=(x_1,x_2)$ along the bonds, for which we adopt here the path that starts from the site 0 and go straight first in the 1 direction and then in the 2 direction reaching the site x when $x_1 x_2 \geqslant 0$, and first in the 2 direction and then in the 1 direction when $x_1 x_2 < 0$.

The improved algorithm of the finite lattice method to generate the high-temperature expansion series for the correlation function of this model is essentially the same as that for the free energy described in Ref. [28]. We first calculate the correlation function for each of the finite-size rectangular lattice $\Lambda(l_1 \times l_2, p)$ with a restricted range of the value of the plaquette variable

$$\langle \vec{s}_x \cdot \vec{s}_0 \rangle_{\Lambda;h_+,h_-} = \frac{\Gamma_{x,0}(\Lambda,h_+,h_-)}{Z(\Lambda,h_+,h_-)}. \tag{13}$$

Here the finite size lattice $\Lambda(l_1 \times l_2, p)$ is specified by its size $|\Lambda| = l_1 \times l_2$ and its position p, and each plaquette variable h_i

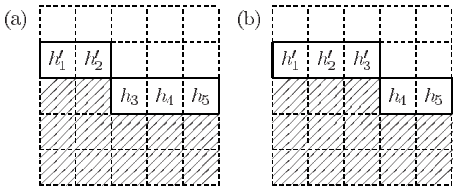

FIG. 1. Intermediate steps in the calculation of $\Gamma_{x,0}(\Lambda,h_+,h_-)$ and $Z(\Lambda,h_+,h_-)$ with the plaquette-by-plaquette construction.

is restricted so that $h_- \leqslant h_i \leqslant h_+$ (where $h_- \leqslant 0$ and $h_+ \geqslant 0$) both in the calculation of the numerator and the denominator. We define the size of the finite lattice so that the $l_1 \times l_2$ lattice involves $l_1 \times l_2$ plaquettes, including the bonds and sites on their boundary. For instance, the 1×1 lattice consists of a single plaquette, including four bonds and four sites. We take into account finite-size lattices with $l_1=0$ and/or $l_2=0$. An $l_1 \times 0$ lattice consists of l_1 bonds and l_1+1 sites with no plaquette. The 0×0 lattice consists only of one site with no bond or plaquette. The boundary condition is taken such that all the plaquette variables outside the $l_1 \times l_2$ lattice are fixed to zero.

The numerator and the denominator of Eq. (13) can be calculated efficiently by the transfer matrix method using a procedure in which a finite-size lattice is built plaquette by plaquette [29,30]. For instance, in the calculation of the denominator $Z(\Lambda,h_+,h_-)$ for the case of $|\Lambda|=5\times 5$, let $z(h'_1,h'_2,h_3,h_4,h_5)$ be the intermediate function which is obtained by summing up for all the plaquette variables in the shaded region in Fig. 1(a) with the set of plaquette variables $\{h'_1,h'_2,h_3,h_4,h_5\}$ on the strip fixed and where $z'(h'_1,h'_2,h'_3,h_4,h_5)$ is the intermediate function which is obtained by summing up for all the plaquette variables on the shaded region in Fig. 1(b) with the set of plaquete variables $\{h'_1,h'_2,h'_3,h_4,h_5\}$ on the strip fixed. Then we can obtain $z'(h'_1,h'_2,h'_3,h_4,h_5)$ by summing with respect to h_3 as

$$z'(h'_1,h'_2,h'_3,h_4,h_5) = \sum_{h_- \leqslant h_3 \leqslant h_+} I_{|h'_3-h'_2|}(\beta) I_{|h'_3-h_3|} \times (\beta) z(h'_1,h'_2,h_3,h_4,h_5). \quad (14)$$

Repeating this procedure gives the total of $Z(\Lambda,h_+,h_-)$. The necessary number of the configurations for the plaquette variables to be kept in each of the intermediate step of the calculation for $Z(\Lambda,h_+,h_-)$ is $(h_+ + |h_-| + 1)^{l_1}$ for the lattice size $|\Lambda|=l_1 \times l_2$.

We then define $\phi_{x,0}(\Lambda,h_+,h_-)$ of the finite size lattice Λ and of the restricted range of the plaquette variables recursively as

$$\phi_{x,0}(\Lambda,h_+,h_-) = \langle \vec{s}_x \cdot \vec{s}_0 \rangle_{\Lambda;h_+,h_-} - \sum_{\substack{\Lambda' \subseteq \Lambda,\ 0 \leqslant h'_+ \leqslant h_+,\ h_- \leqslant h'_- \leqslant 0 \\ (\Lambda',h'_+,h'_-) \neq (\Lambda,h_+h_-)}} \phi_{x,0}(\Lambda',h'_+,h'_-). \quad (15)$$

It should be noted that $\phi_{x,0}(\Lambda,h_+,h_-)=0$ if the site x or 0 is not included in Λ.

The correlation function in the thermodynamic limit is then given by

$$\langle \vec{s}_x \cdot \vec{s}_0 \rangle \equiv \lim_{|\Lambda| \to \infty,\ h_+ \to \infty,\ h_- \to -\infty} \langle \vec{s}_x \cdot \vec{s}_0 \rangle_{\Lambda;h_+,h_-} = \sum_{\Lambda,h_+,h_-} \phi_{x,0}(\Lambda,h_+,h_-). \quad (16)$$

In the last line of Eq. (16) the summation should be taken for all the lattice sizes and all of their positions and all integer values of h_+ and h_- with $0 \leqslant h_+ \leqslant \infty$, $-\infty \leqslant h_- \leqslant 0$.

In the standard (graphical) cluster expansion of the correlation function for the SOS model, a cluster is composed of polymers: one main polymer that consists of the set of bonds $L_{x,0}$ and connected plaquettes attaching to it and possible subpolymers that consists of connected plaquettes. An example of the main polymer and subpolymer can be seen in Fig. 1. A value $h_i(\neq 0)$ is assigned to each plaquette i of the polymer. We can assign to each cluster two numbers $h_{\max}(\geqslant 0)$ and $h_{\min}(\leqslant 0)$, which are the maximum and the minimum, respectively, of the plaquette variable h_i in all the plaquettes of the polymers of which the cluster consists. Then, we can prove [16] that $\phi_{x,0}(\Lambda,h_+,h_-)$ includes the contributions to $\langle \vec{s}_x \cdot \vec{s}_0 \rangle$ from all the clusters of polymers in the standard cluster expansion for which $h_{\max}=h_+$ and $h_{\min}=h_-$ and that can be embedded into the lattice Λ but cannot be embedded into any of its rectangular sublattices.

Now we consider from what order the series expansion of $\phi_{x,0}(\Lambda,h_+,h_-)$ with respect to β starts. It is enough to give the order for the position $x=(x_1,x_2)$ so that $x_1 \geqslant 0$ and $x_2 \geqslant 0$. The order for the other cases is known by the 90° rotational symmetry of the model. Any cluster that contributes to the lowest-order term of the series expansion for $\phi_{x,0}(\Lambda,h_+,h_-)$ consists only of a main polymer. Hence the series expansion of $\phi_{x,0}(\Lambda,h_+,h_-)$ begins from order $\beta^{n_{x,0}(\Lambda,h_+,h_-)}$ in the case of $h_+ \geqslant 1$ and $h_- \leqslant -1$ with

$$n_{x,0}(\Lambda,h_+,h_-) = \begin{cases} 2l_1 + 2l_2 - x_1 - x_2 + 4h_+ + 4|h_-| - 4 & \text{for } (p_1,p_2) = (0,0) \text{ and } (p'_1,p'_2) = (x_1,x_2), \\ 2l_1 + 2l_2 - x_1 - x_2 + 4h_+ + 4|h_-| - 6 & \text{for } p_2 = 0,\ p'_1 = x_1 \text{ and } (p_1,p'_2) \neq (0,x_2), \\ 2l_1 + 2l_2 - x_1 - x_2 + 4h_+ + 4|h_-| - 8 & \text{for the others.} \end{cases} \quad (17)$$

Here we denote (p_1,p_2) as the position of the bottom-left corner and (p'_1,p'_2) as the position of the top-right corner, respectively, of the lattice Λ with its size $l_1 \times l_2$ ($p'_1-p_1=l_1$ and $p'_2-p_2=l_2$). Examples of the main polymer are given in Figs. 2(a)–2(c), which correspond to the three cases in Eq. (17), respectively. In the case of $h_+ \geqslant 1$ and $h_-=0$ we have

$$n_{x,0}(\Lambda,h_+,h_-)=\begin{cases}2l_1+2l_2-x_1-x_2+4h_+ & \text{for } p_1=0,\ p_2'=x_2, \text{ and } (p_2,p_1')\neq(0,x_1),\\ 2l_1+2l_2-x_1-x_2+4h_+-2 & \text{for } p_1=0,\ p_2<0, \text{ and } (p_2'>x_2 \text{ or } p_1'=x_1),\\ 2l_1+2l_2-x_1-x_2+4h_+-2 & \text{for } p_2'=x_2,\ p_1'>x_1 \text{ and } [p_1<0 \text{ or } (p_1,p_2)=(0,0)],\\ 2l_1+2l_2-x_1-x_2+4h_+-4 & \text{for the others}\end{cases} \tag{18}$$

and in the case of $h_+=0$ and $h_-\leqslant -1$

$$n_{x,0}(\Lambda,h_+,h_-)=\begin{cases}2l_1+2l_2-x_1-x_2+4|h_-| & \text{for } (p_1,p_2)=(0,0) \text{ and } (p_1',p_2')=(x_1,x_2),\\ 2l_1+2l_2-x_1-x_2+4|h_-|+4 & \text{for } p_2=0,\ p_1'=x_1 \text{ and } (p_1,p_2')\neq(0,x_2),\\ 2l_1+2l_2-x_1-x_2+4|h_-| & \text{for } p_2=0,\ p_1<0 \text{ or } p_1'=x_1,\ p_2'>x_2,\\ 2l_1+2l_2-x_1-x_2+4|h_-|-4 & \text{for the others.}\end{cases} \tag{19}$$

Examples of the main polymer are given in Figs. 3(a) and 3(b), which correspond to the last case in Eq. (18) and the last case in Eq. (19), respectively. In the case of $h_+=0$ and $h_-=0$ we have

$$n_{x,0}(\Lambda,h_+,h_-)=\begin{cases}l_1+l_2 & \text{for } (p_1,p_2)=(0,0) \text{ and } (p_1',p_2')=(x_1,x_2),\\ \infty & \text{for the others.}\end{cases} \tag{20}$$

Here $n_{x,0}(\Lambda,h_+,h_-)=\infty$ implies that $\phi_{x,0}(\Lambda,h_+,h_-)=0$. Thus, in order to obtain the expansion series for the correlation function $\langle\vec{s}_x\cdot\vec{s}_0\rangle$ to order β^N, we have only to take into account all combinations of the rectangular lattice Λ and the range of the plaquette variable (h_+,h_-) that satisfy the relation $n_{x,0}(\Lambda,h_+,h_-)\leqslant N$ in the summation of Eq. (16) and to evaluate each of the $\phi_{x,0}(\Lambda,h_+,h_-)$ to order β^N.

The jth moment of the correlation function is given by

$$m_j=\sum_x |x|^j\langle\vec{s}_x\cdot\vec{s}_0\rangle, \tag{21}$$

where $|x|$ is the distance between the site x and 0. The moment can be calculated more efficiently in the following way. First we calculate $\tilde{\Gamma}_j(l_1,l_2,h_+,h_-)$ defined by

$$\tilde{\Gamma}_j(l_1,l_2,h_+,h_-)=\frac{\Sigma_{x,y\subseteq\Lambda}|x-y|^j\Gamma_{x,y}(\Lambda,h_+,h_-)}{Z(\Lambda)} \tag{22}$$

for each finite size lattice Λ. We note that the numerator and the denominator of Eq. (22) depend only on the lattice size $|\Lambda|=l_1\times l_2$ and on h_+,h_- and that they are independent of the position of the lattice after the summation is taken for x and y. They can be calculated efficiently again by the transfer matrix method using the procedure in which a finite-size lattice is built one plaquette at a time not only for $j=0$ but also for $j\geqslant 2$ (j:even), the detail of which was described in the application of the finite lattice method to the calculation of the low-temperature series for the second moment of the correlation function in the simple cubic Ising model [22]. The moment is then given by

$$m_j=\sum_{l_1,l_2,h_+,h_-}\tilde{\phi}_j(l_1,l_2,h_+,h_-), \tag{23}$$

where $\tilde{\phi}_j(l_1,l_2,h_+,h_-)$ is defined recursively as

$$\tilde{\phi}_j(l_1,l_2,h_+,h_-)=\tilde{\Gamma}_j(l_1,l_2,h_+,h_-)-\sum_{\substack{l_1',l_2',h_+',h_-'\\(l_1',l_2',h_+',h_-')\neq(l_1,l_2,h_+,h_-)}}(l_1-l_1'+1)\times(l_2-l_2'+1)\tilde{\phi}_j(l_1',l_2',h_+',h_-'). \tag{24}$$

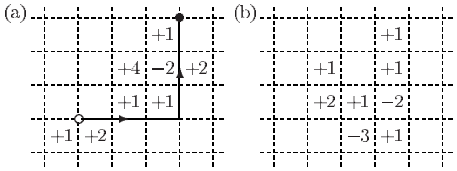

FIG. 2. (a) Example of the main polymer in the standard cluster expansion. The open circle indicates the site (0,0) where the spin $\vec{s}_0$ exists and the closed circle indicates the site $x=(x_1,x_2)$ where the spin $\vec{s}_x$ exists. (b) Example of the subpolymer.

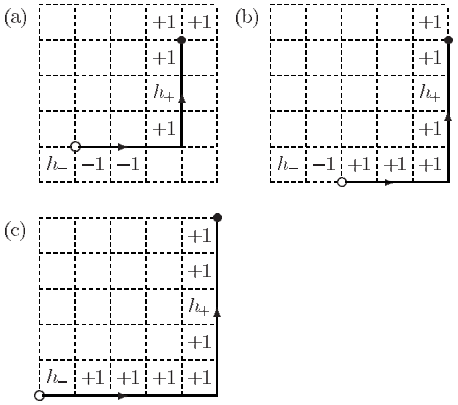

FIG. 3. Examples of the cluster composed of a single main polymer that contributes to the lowest order term of the high-temperature expansion of $\phi(\Lambda,h_+,h_-)$ for $h_+\geqslant 1$ and $h_-\leqslant -1$. The size of the finite lattices in these examples is $|\Lambda|=5\times 5$.

TABLE I. Coefficients of the high-temperature series for the magnetic susceptibility m_0.

n	$a_n^{(0)}$		
0	1	/	1
1	4	/	1
2	12	/	1
3	34	/	1
4	88	/	1
5	658	/	3
6	529	/	1
7	14933	/	12
8	5737	/	2
9	389393	/	60
10	2608499	/	180
11	3834323	/	120
12	1254799	/	18
13	84375807	/	560
14	6511729891	/	20160
15	66498259799	/	96768
16	1054178743699	/	725760
17	39863505993331	/	13063680
18	19830277603399	/	3110400
19	8656980509809027	/	653184000
20	2985467351081077	/	108864000
21	811927408684296587	/	14370048000
22	399888050180302157	/	3448811520
23	245277792666205990697	/	1034643456000
24	83292382577873288741	/	172440576000
25	37698897018959709058 7	/	384296140800
26	62337378385915430773643	/	31384184832000
27	480555032864478422139959	/	119830523904000
28	80636088313579215330647	/	9985876992000
29	19240186846097940775812460721	/	1186322186649600000
30	34266867760374182809422566317	/	1054508610355200000
31	98642320023286158917622210699 59	/	151849239891148800000
32	93697376428024822547085555709	/	723091618529280000
33	66586187862651970031739824929 1449	/	2581437078149529600000

From Eqs. (17)–(20) we know that $\tilde{\phi}_j(l_1,l_2,h_+,h_-)$ starts from order $\beta^{\tilde{n}(l_1,l_2,h_+,h_-)}$ with

$$\tilde{n}(l_1,l_2,h_+,h_-) = \begin{cases} l_1+l_2 & \text{for } h_+=h_-=0, \\ l_1+l_2+4h_+-4 & \text{for } h_+>0 \text{ and } h_-=0, \\ l_1+l_2+4|h_-|-3 & \text{for } h_+=0 \text{ and } h_-<0, \\ l_1+l_2+4h_++4|h_-|-7 & \text{for } h_+>0 \text{ and } h_-<0. \end{cases} \tag{25}$$

III. SERIES

We have calculated the high-temperature expansion series to order β^{33} for the jth moments m_j $(j=0,2,4)$ of the correlation function for the XY model on the square lattice (m_0 is the magnetic susceptibility). The obtained expansion coefficients are listed in Tables I–III, where the coefficient $a_n^{(j)}$ is defined as

$$m_j = \sum_{n=1}^{N} a_n^{(j)} \left(\frac{\beta}{2}\right)^n. \tag{26}$$

We have checked that each of the $\tilde{\phi}_j(l_1,l_2;h_+,h_-)$'s in Eq. (24) starts from the correct order in β, as given by Eq. (25). Our series coincide exactly with the series to order β^{21} for $j=0$, 2 and 4 given by Campostrini *et al.* [7] and to order β^{26} for $j=0$ and 2 given by Butera and Pernici [8,31], which was obtained by a graphical method and a nongraphical recursive

TABLE II. Coefficients of the high-temperature series for the second moment m_2 of the correlation function.

n	$a_n^{(2)}$		
0	0	/	1
1	4	/	1
2	32	/	1
3	162	/	1
4	672	/	1
5	7378	/	3
6	24772	/	3
7	312149	/	12
8	77996	/	1
9	13484753	/	60
10	28201211	/	45
11	611969977	/	360
12	202640986	/	45
13	58900571047	/	5040
14	3336209179	/	112
15	1721567587879	/	23040
16	16763079262169	/	90720
17	5893118865913171	/	13063680
18	17775777329026559	/	16329600
19	1697692411053976387	/	653184000
20	41816028466101527	/	6804000
21	206973837048951639371	/	14370048000
22	72161768129501978 2781	/	21555072000
23	79897272060888843617033	/	1034643456000
24	2287397511857949924319	/	12933043200
25	5412508223507386985733313	/	13450364928000
26	7139182711315236460182251	/	7846046208000
27	10785199506434607033 6358789	/	52725430517760
28	7535589521452859522 6953733	/	16476697036800
29	17240761920913139729 41261252343	/	169474598092800000
30	53429382179619216000735913825117	/	2372644373299200000
31	75346092479916805701130557331782 47	/	151849239891148800000
32	34437336382398536032696170120 7501	/	3163525831065600000
33	68217033997582723452684940622596049	/	2868263420166144000 00

algorithm based on the Schwinger-Dyson equations, respectively.

To obtain the large numerators and denominators of the coefficients exactly, we have used the same technique as in the calculation of the free energy series [28]. In each step of the calculation the series expansion of a function $f(\beta)$ is expressed as

$$f(\beta) = \sum_n \frac{a_n}{n!}\left(\frac{\beta}{2}\right)^n, \quad g(\beta) = \sum_n \frac{b_n}{n!}\left(\frac{\beta}{2}\right)^n, \tag{27}$$

then the product of the two functions is given by

$$f(\beta)g(\beta) = \sum_n \frac{c_n}{n!}\left(\frac{\beta}{2}\right)^n, \tag{28}$$

with

$$c_n = \sum_{n'=0}^{n} \frac{n!}{n'!(n-n')!} a_{n'} b_{n-n'}, \tag{29}$$

and, if a_n's and b_n's are integers, c_n's are also integers.

The calculations were carried out on a PC cluster at the Information Processing Center at OPCT and on an Altix3700 BX2 at Yukawa Institute of Kyoto University. Each CPU of these computers was used as stand alone (not parallelized). A

TABLE III. Coefficients of the high-temperature series for the fourth moment m_4 of the correlation function.

n	$a_n^{(4)}$		
0	0	/	1
1	4	/	1
2	96	/	1
3	930	/	1
4	6112	/	1
5	96850	/	3
6	147648	/	1
7	7305173	/	12
8	2319540	/	1
9	498173873	/	60
10	1271029508	/	45
11	2210163319	/	24
12	2606525954	/	9
13	4449953438647	/	5040
14	3300804041221	/	1260
15	81597010130527	/	10752
16	1952458419167723	/	90720
17	782261299458533011	/	13063680
18	222847854860540393	/	1360800
19	287995465331747559427	/	653184000
20	15925021359550756357	/	13608000
21	8810941751514830879983	/	2874009600
22	8551911058786623741001	/	1077753600
23	2101354818423820807059863 3	/	1034643456000
24	1108989303528609120610577	/	21555072000
25	3156697598264892600519355 9	/	244552089600
26	6295468098752045929619455 33	/	1961511552000
27	1043070737244084798242371813021	/	1318135762944000
28	1063125380506276139105680 6729	/	5492232345600
29	5575566587216452758709818963741041	/	1186322186649600000
30	2240485100208335200628893992637883	/	197720364441600000
31	6340392520271196292461573024022 7527	/	2336142152171520000
32	8174296006615548272296498779225887	/	126541033242624000
33	3945478959328472114701692062051549583 61	/	2581437078149529600000

maximum memory of 8 Gb was used for each CPU and the total CPU time used by the computers was about 15 000 h.

IV. SERIES ANALYSIS

From Eq. (3) the logarithm of the moment of the correlation function is expected to behave near the critical temperature as

$$\ln m_j \sim \frac{(2+j-\eta)b}{\tau^{\sigma}} + O(\ln \tau), \tag{30}$$

where $\tau=1-\beta/\beta_c$ and $\beta_c=J/kT_c$ is the critical inverse temperature. Here we analyze it by the first order inhomogeneous differential approximation (IDA), in which the differential equation for $f(\beta)=\ln m_j$ is satisfied as

$$Q_m(\beta)f'(\beta) + P_l(\beta)f(\beta) + R_k(\beta) = O(\beta^{m+l+k+2}), \tag{31}$$

where $Q_m(\beta)$, $P_l(\beta)$, and $R_k(\beta)$ are polynomials of order m, l, and k, respectively, and $Q_m(0)=1$. The critical inverse temperature β_c is given by the zero of $Q_m(\beta)$ and the exponent σ is evaluated by

$$\sigma = -\frac{P_l(\beta_c)}{Q_m'(\beta_c)}. \tag{32}$$

In the analysis by the first order IDA here and below, we restrict $m+l+k+2$ to be the maximum order of the analyzed series with $-1 \leqslant k \leqslant 9$ and $|m-l| \leqslant 4$, and exclude the approximants that have another zero of $Q_m(\beta)$ with $|\beta-\beta_c|/\beta_c < 0.10$, which is called near-by singularity.

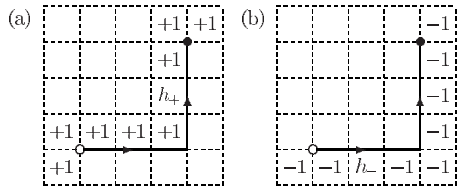

FIG. 4. Examples of the cluster composed of a single main polymer that contributes to the lowest order term of the high-temperature expansion of $\phi(\Lambda,h_+,h_-)$ (a) for $h_+\geqslant 1$ and $h_-=0$ and (b) for $h_+=0$ and $h_-\leqslant -1$. The size of the finite lattice in these examples is $|\Lambda|=5\times 5$.

In Fig. 4 we plot the zeros of $Q_m(\beta)$ in the complex plane of β. (We have plotted the zeros only for the approximants with $-1\leqslant k\leqslant 9$ and $|m-l|\leqslant 2$, so that the relative density of the zeros would be visualized properly.) In addition to clear accumulation of the points around $\beta=1.12$ we see another dense accumulation around the nonphysical point $\beta=\beta_0 \sim -1.2\pm 0.2i$. In order to remove the influence of these nonphysical singularities, we have made Euler transformation

$$\beta' = \frac{\beta}{1-\beta/\beta_0} \tag{33}$$

with $\beta_0=-1.2$. In fact after this transformation the IDA gives a series of (β_c,σ) which converges much better onto a straight line. Biased analysis fixing $\sigma=\frac{1}{2}$ gives $\beta_c=1.1200(4)$. Hence we apply this Euler transformation in all of the series analysis presented below.

The above analysis ignores the existence of the subleading correction terms to the leading power-law singularity of $\ln m_j$ in Eq. (30). So we have analyzed a combination of m_0 and m_2 as

$$\ln m_0 + c \ln \frac{m_2}{4\beta}, \tag{34}$$

searching the parameter c which will give better converged result, anticipating that the subleading terms will be cancelled between the first and second terms in Eq. (34). For the biased analysis fixing $\sigma=\frac{1}{2}$, the choice of the parameter $c=0.08-0.12$ gives nicely converging result of $\beta_c=1.12007(4)$. We have also analyzed other combinations as

$$\ln m_0 + c_j' \ln\left(1 + c_j'' \frac{m_2}{m_0^j}\right), \tag{35}$$

with $j=0$, 1, and 2, where c_j' and c_j'' are arbitrary parameters which should be chosen so that the combination will give the best converged result. We have obtained the best converged result of $\beta_c=1.12006(6)$ around $c_1'=0.07$ and $c_1''=1.9$ for $j=1$; $\beta_c=1.12003(5)$ around $c_2'=0.05$ and $c_2''=0.58$; and $\beta_c=1.11997(5)$ around $c_2'=0.03$ and $c_2''=0.68$ for $j=2$. The above results are obtained for the series for m_0 and m_2 to order β^{33}. The best converged results of the combined quantities for almost the same values of the parameter c in Eq. (34) and c_j' and c_j'' in Eq. (35) are also observed for the series to order β^N with $30\leqslant N\leqslant 32$, while we do not find any parameter c or c_j' and c_j'' that improves the convergence so much for the series with $N\leqslant 29$. Unfortunately we do not know the reason for the latter by now and it could be clarified by investigating even higher order series. As for the combination with $j=0$ in Eq. (35), no well converged result around special values of the parameters c_0' and c_0'' such as the cases of $j=1$ and 2 is obtanined. In this case almost all of the inhomogeneous differential approximants for the second term alone and also for the combination of the first and the second terms have one or more singularities closer to the origin on the real axis in addition to the singularity at $\beta=\beta_c\sim 1.12$. On the other hand, most of the approximants for the combination in Eq. (34) and for the combination in Eq. (35) with $j=1$ and 2 do not have such an singularity closer to the origin. These might be the reason why the combination (35) with $j=0$ does not give well converged result. Anyhow the best converged values for the three types of the combinations described above are within the range of $\beta_c=1.1200(1)$. This value is quite consistent with the most precise value $\beta_c=1.1199(1)$ obtained by Hasenbusch from the large-scale Monte Carlo simulation [6]. Our value is much more precise than the value $\beta_c=1.1198(14)$ by Butera and Pernici [8,31] from the high-temperature series to order β^{26}.

Assuming the critical behavior of Eqs. (1) and (3) we can estimate the nonuniversal parameter b by the Padé approximation of

$$\left(1-\frac{\beta}{\beta_c}\right)^{1/2} \ln\left(1 + c\frac{m_2}{m_0}\right) \sim b \tag{36}$$

and

$$\left(1-\frac{\beta}{\beta_c}\right)^{1/2} \ln\left(1 + c'\frac{m_4}{m_2}\right) \sim b. \tag{37}$$

By searching the parameter c or c' that gives the best converged estimation of b keeping $\beta_c=1.12000$ and $\sigma=\frac{1}{2}$, both of the two give the same result of $b=1.758(1)$ for $c=3.15-3.23$ and for $c'=0.806-0.812$, respectively. Here we have used all of $[m,l]$ Padé approximants with $m\geqslant 14$ and $l\geqslant 14$. This value is a bit smaller than $b=1.800(2)$ [4] and $b=1.776(4)$ [5] obtained in the Monte Carlo simulations.

Unfortunately the long series do not improve the estimation of the exponent η so much. For instance, the Padé approximation of the quantities

$$\frac{\ln\left(1 + c\frac{m_2}{m_0}\right)}{\ln m_0} \sim \frac{2}{2-\eta} \tag{38}$$

and

$$\frac{\ln\left(1 + c'\frac{m_2}{m_0^2}\right)}{\ln m_0} \sim \frac{\eta}{2-\eta} \tag{39}$$

give the best converged result of $\eta=0.256(2)$ for $c=0.69$ and $\eta=0.227(2)$ for $c'=0.60$, respectively. The Padé approximation of

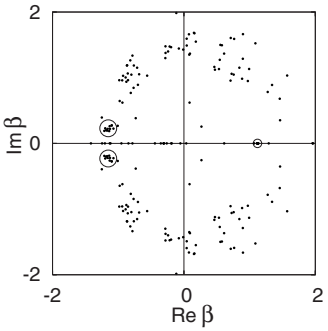

FIG. 5. Plot of poles in the unbiased inhomogeneous deferential approximation for $\ln m_0$. The small open circle indicates the poles corresponding to the physical singularity and the two large open circles indicate the accumulation of nonphysical poles.

$$\left(1-\frac{\beta}{\beta_c}\right)^{1/2}\ln\left(1+c''\frac{m_2}{m_0^2}\right)\sim \eta b \tag{40}$$

gives $\eta b=0.429(5)$ for $c''=0.83-0.89$ and, if we combine this with the above result $b=1.758(1)$, gives $\eta=0.244(3)$

As for the exponent θ, Dlog-Padé analysis of the 20th order series of the quantities

$$\frac{m_0}{\left(\frac{m_2}{m_0}\right)^{2-\eta}}\sim\frac{m_4}{\left(\frac{m_2}{m_0}\right)^{6-\eta}}\sim\tau^{-2\sigma\theta}\{1+O(\tau^{\sigma}\ln\tau)\} \tag{41}$$

gave estimations $\theta=-0.042(5)$ and $\theta=-0.05(2)$ [7], which have the opposite sign to the renormalization group prediction of $\theta=\frac{1}{16}$. The situation does not change even if our long series are used in the Dlog-Padé analysis of these quantities. The series of the two quantities to 33rd order gives $\theta=-0.019(1)$ and $\theta=-0.015(9)$, respectively. The IDA with $k\geqslant 0$ gives rather convergent values within the same k but quite scattered values for different k's.

One possible reason why IDA for these quantities give scattered values for different k may be the existence of the subleading logarithmically singular term in Eq. (41), which comes from the correction factor in Eq. (3). In fact the subleading logarithmic singularity can strongly disturb the correct evaluation of the leading power low exponent $2\sigma\theta$ if this exponent is as small as $\frac{1}{16}$. We plot in Fig. 5 the estimated value of θ by IDA for the expansion series to order β^{33} for a test function

$$\tau^{-2\sigma\theta}\{1+\tau^{\sigma}(A+B\ln\tau)\} \tag{42}$$

with $\theta=\frac{1}{16}$, $\sigma=\frac{1}{2}$, and $A=0$ plotted versus B. We find that the estimated value of θ is quite sensitive to the amplitude B of the logarithmic term, and although each approximant with the same k gives rather convergent result for any fixed value of B, the approximants with different k give the estimation of θ far from each other.

Thus we have evaluated θ using the combination of m_0, m_2 and m_4 as

$$m_0{}^{\alpha}(1+c'm_2)^{\alpha'}(1+c''m_4)^{\alpha''} \tag{43}$$

with

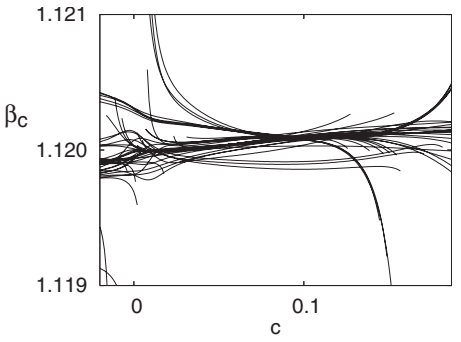

FIG. 6. β_c given by the biased IDA for $\ln m_0+c\ln\frac{m_2}{4\beta}$.

$$\alpha(2-\eta_0)+\alpha'(4-\eta_0)+\alpha''(6-\eta_0)=0 \tag{44}$$

and

$$\alpha+\alpha'+\alpha''=1 \tag{45}$$

and $\eta_0=\frac{1}{4}$, which is also considered to behave similar to Eq. (42) in general. We can, however, anticipate that, by taking the combination of the three quantities, the subleading logarithmic term may be cancelled if we choose appropriate values for the parameters α, c' and c''. We have used the biased second-order IDA;

$$\tau^2 Q_{m_2}(\beta)f''(\beta)+\tau Q_{m_1}(\beta)f'(\beta)+P_l(\beta)f(\beta)+R_k(\beta) = O(\beta^{m_2+m_1+l+k+3}) \tag{46}$$

with $Q_{m_2}(0)=1$. The exponent $-2\sigma\theta$ can be evaluated by the solution γ of

$$\gamma(\gamma-1)\frac{Q_{m_2}(\beta_c)}{\beta_c{}^2}-\gamma\frac{Q_{m_1}(\beta_c)}{\beta_c}+P_l(\beta_c)=0. \tag{47}$$

Here we adopt $\beta_c=1.1200$. The second-order IDA can make more precise evaluation of θ than the first-order IDA for a function such as Eq. (42). Figure 6 is the plot of the estimation of θ by the second-order IDA for the 33rd-order series of the test function (42) with $\theta=\frac{1}{16}$, $\sigma=\frac{1}{2}$, and $A=0.3$. Of course the second-order IDA also gives different values of θ for each of k if $B\neq 0$, but if B is small enough it can present precise estimation for the exponent of the leading singularity. By the analysis of the real combined quantity (43) we have found that the estimated values of θ converge to $\theta=0.050(15)$ for all the range of $-1\leqslant k\leqslant 9$ in a domain of the

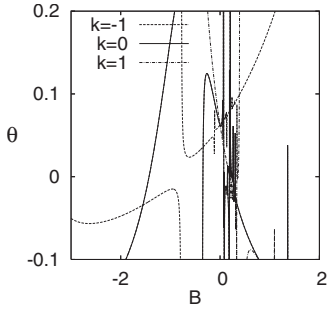

FIG. 7. Plot of the estimated value of θ by the first-order IDA for the test function versus B.

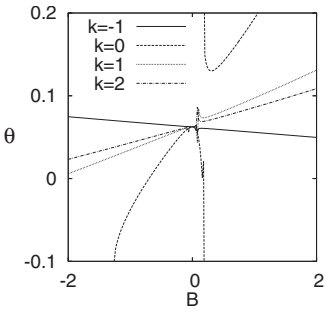

FIG. 8. Plot of the estimated value of θ by the second-order IDA for the test function versus B.

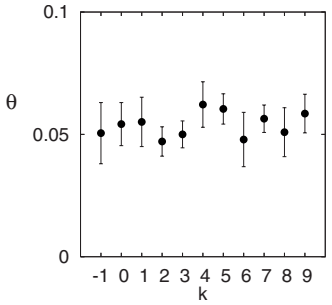

FIG. 9. Value of θ for each of k estimated by the second-order IDA of the combined quantity.

set of parameters $-\alpha=3.6-3.0$, $c'=2.8-4.0$, and $c''=2.8-4.0$. In the analysis we have restricted $m_2+m_1+l+k+3=32$ with $-1\leqslant k\leqslant 9$ and $m_2\geqslant 7$, $m_1\geqslant 7$, $l\geqslant 7$. The approximants that have near-by singularity [i.e., the zero of $Q_2(\beta)$ or $Q_1(\beta)$] with $|\beta-\beta_c|/\beta_c<0.2$ have been excluded. The best converged result $\theta=0.054(10)$ is obtained for $\alpha=-3.143$, $c'=3.134$, and $c''=3.139$. The values of θ for each k in this set of parameters are shown in Figs. 7–9. We note that this value $\theta=0.054(10)$ is consistent with $\theta=\frac{1}{16}$ predicted by the renormalization group.

V. SUMMARY

We calculated the high-temperature series for the zeroth moment (magnetic susceptibility) and the second and fourth moments of the correlation function in the XY model on the square lattice to order β^{33} by using the improved algorithm of the finite lattice method. The long series has presented us an estimation for the value of the critical inverse temperature as $\beta_c=1.1200(1)$, which is consistent with the most precise value given previously by the Monte Carlo simulation. The critical exponent θ for the multiplicative logarithmic correction is evaluated using the combination of the three moments of the correlation function, giving $\theta=0.054(10)$, which is consistent with the value $\theta=\frac{1}{16}$ predicted by the renormalization group argument.

ACKNOWLEDGMENTS

The author would like to thank P. Butera and M. Pernici for sending their high-temperature series before publication. This work was supported in part by a Grant-in-Aid for Scientific Research (Grant No. 16540353) from the Ministry of Education, Culture, Sports, Science and Technology.

[1] J. M. Kosterlitz and D. J. Thouless, J. Phys. C **6**, 1181 (1973); J. M. Kosterlitz, *ibid.* **7**, 1046 (1974).
[2] R. G. Edwards, J. Goodman, and A. D. Sokal, Nucl. Phys. B **354**, 289 (1991).
[3] P. Majumdar, Phys. Rev. D **45**, 2883 (1992).
[4] N. Schultka and E. Manousakis, Phys. Rev. B **49**, 12071 (1994).
[5] M. Hasenbusch and K. Pinn, J. Phys. A **30**, 63 (1997).
[6] M. Hasenbusch, J. Phys. A **38**, 5869 (2005).
[7] M. Campostrini, A. Pelissetto, P. Rossi, and E. Vicari, Phys. Rev. B **54**, 7301 (1996).
[8] P. Butera and M. Pernici, Physica A **387**, 6293 (2008).
[9] A. Patrascioiu and E. Seiler, Phys. Rev. B **54**, 7177 (1996).
[10] W. Janke, Phys. Rev. B **55**, 3580 (1997).
[11] A. Jaster and H. Hahn, Physica A **252**, 199 (1998).
[12] R. Kenna and A. C. Irving, Nucl. Phys. B **485**, 583 (1997).
[13] S. Chandrasekharan and C. G. Strouthos, Phys. Rev. D **68**, 091502(R) (2003); C. G. Strouthas, Nucl. Phys. B (Proc. Suppl.) **129**, 608 (2004).
[14] See, for example, C. Domb, in *Phase Transitions and Critical Phenomena*, edited by C. Domb and M. S. Green (Academic, London, 1974), Vol. 3, Chap. 1, 6.
[15] T. de Neef and I. G. Enting, J. Phys. A **10**, 801 (1977); I. G. Enting, *ibid.* **11**, 563 (1978); Aust. J. Phys. **31**, 515 (1978).
[16] H. Arisue and T. Fujiwara, Prog. Theor. Phys. **72**, 1176 (1984); Report No. RIFP-588 (unpublished); H. Arisue, Nucl. Phys. B (Proc. Suppl.) **34**, 240 (1994).
[17] M. Creutz, Phys. Rev. B **43**, 10659 (1991).
[18] G. Bhanot, M. Creutz and J. Lacki, Phys. Rev. Lett. **69**, 1841 (1992); G. Bhanot, M. Creutz, U. Glässner, and K. Schilling, Phys. Rev. B **49**, 12909 (1994).
[19] A. J. Guttmann and I. G. Enting, J. Phys. A **26**, 807 (1993); **27**, 1503 (1994).
[20] H. Arisue, Phys. Lett. B **313**, 187 (1993).
[21] H. Arisue and T. Fujiwara, Nucl. Phys. B **285**, 253 (1987); H. Arisue, Phys. Lett. B **322**, 224 (1994).
[22] H. Arisue and K. Tabata, Nucl. Phys. B **435**, 555 (1995).
[23] G. Bhanot, M. Creutz, U. Glässner, I. Horvath, J. Lacki, K. Schilling, and J. Weckel, Phys. Rev. B **48**, 6183 (1993).
[24] A. J. Guttmann and I. G. Enting, J. Phys. A **27**, 5801 (1994).
[25] H. Arisue, Phys. Rev. E **59**, 186 (1999); Nucl. Phys. B **546**, 558 (1999).
[26] H. Arisue and K. Tabata, Nucl. Phys. B **446**, 373 (1995).
[27] H. Arisue and K. Tabata, J. Phys. A **30**, 3313 (1995).
[28] H. Arisue, Prog. Theor. Phys. **118**, 855 (2007).
[29] I. G. Enting, J. Phys. A **13**, 3713 (1980).
[30] G. Bhanot, J. Stat. Phys. **60**, 55 (1990).
[31] P. Butera and M. Pernici, Phys. Rev. B **76**, 092406 (2007).